SUPPORTING INFORMATION

Multifunctional Switch Mediates Catalytic Activity and Product Ratio in Fungal CYP512W2

Hanbing Li[a,#], Yuhuan Luo[a,#], Zeqian Du[a], Jian-Jiang Zhong[a], Han Xiao[a,*] and Ting Shi[a,*]
[a]State Key Laboratory of Microbial Metabolism, and School of Life Sciences & Biotechnology,
Shanghai Jiao Tong University, 800 Dong-chuan Road, Shanghai, 200240, China
E-mail: Shi, T. (tshi@sjtu.edu.cn); Xiao, H. (smallhan@sjtu.edu.cn).

Table of Contents

Supporting Figures 3

Figure S1. The ΔΔG value of all mutations (7x19) calculated by FoldX and I-Mutant. 3

Figure S2. The 46 mutations with ΔΔG value less than -2.0 kcal/mol 3

Figure S3. Mutations at L294 and I364 with different residue properties was screened 4

Figure S4. The PCA results of C11-HLDOA-WT/I108A/S/G systems 5

Figure S5. The active pocket of WT and mutants I108A/S/G 6

Figure S6. The PCA results of the substrate GA-Y in WT and mutants I108A/S/G and the corresponding representative conformations 7

Figure S7. Comparative analysis of GA-Y substrate conformation and C15-Hα-O angular distribution 8

Figure S8. Binding mode of HLDOA substrates in C11-HLDOA-I108N complex and dynamic analysis of key parameters 9

Figure S9. The energy decomposition analysis of the C7-HLDOA-I108N complex (a) and the C11-HLDOA-I108N complex (b) 10

Figure S10. The PCA results of the substrate GA-Y in mutant I108N and the PRSs occupancy of C15 site of GA-Y in mutant I108 11

Figure S11. Computational analysis of the C7 radical intermediate in the I108N mutant. 12

Figure S12. The major cluster conformations of (a) I364C and (b) I364H in complex with substrate HLDOA. 13

Figure S13. The yields and product ratios of the combinatorial mutagenesis by shake flask fermentation of strains for 120 h 13

Supporting Tables 14

Table S1. The binding energy and C-O(heme) distance of CYP512W2 mutants' dock results 14

Table S2. Construction of plasmids 15

Table S3. Strains used in this study 20

Table S4. Product ratio of Diverse Mutants to Generate GA-Jb and GA-Y 21

Table S5. The percentage of PRSs in three MD simulations in WT and its variants I108A/S/G 22

Table S6. The binding energy of CYP512W2 mutants calculated by MM/GBSA 22

Supporting Figures

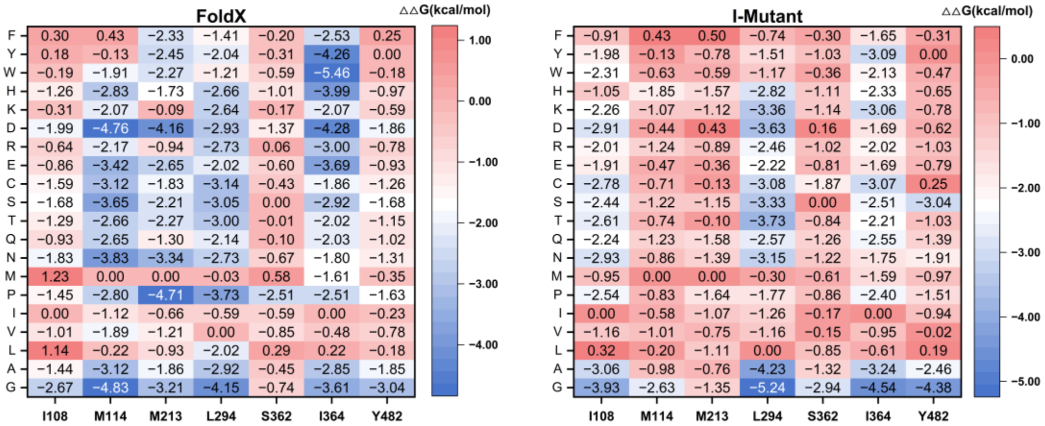

FoldX

	I108	M114	M213	L294	S362	I364	Y482
F	0.30	0.43	−2.33	−1.41	−0.20	−2.53	0.25
Y	0.18	−0.13	−2.45	−2.04	−0.31	−4.26	0.00
W	−0.19	−1.91	−2.27	−1.21	−0.59	−5.46	−0.18
H	−1.26	−2.83	−1.73	−2.66	−1.01	−3.99	−0.97
K	−0.31	−2.07	−0.09	−2.64	−0.17	−2.07	−0.59
D	−1.99	−4.76	−4.16	−2.93	−1.37	−4.28	−1.86
R	−0.64	−2.17	−0.94	−2.73	0.06	−3.00	−0.78
E	−0.86	−3.42	−2.65	−2.02	−0.60	−3.69	−0.93
C	−1.59	−3.12	−1.83	−3.14	−0.43	−1.86	−1.26
S	−1.68	−3.65	−2.21	−3.05	0.00	−2.92	−1.68
T	−1.29	−2.66	−2.27	−3.00	−0.01	−2.02	−1.15
Q	−0.93	−2.65	−1.30	−2.14	−0.10	−2.03	−1.02
N	−1.83	−3.83	−3.34	−2.73	−0.67	−1.80	−1.31
M	1.23	0.00	0.00	−0.03	0.58	−1.61	−0.35
P	−1.45	−2.80	−4.71	−3.73	−2.51	−2.51	−1.63
I	0.00	−1.12	−0.66	−0.59	−0.59	0.00	−0.23
V	−1.01	−1.89	−1.21	0.00	−0.85	−0.48	−0.78
L	1.14	−0.22	−0.93	−2.02	0.29	0.22	−0.18
A	−1.44	−3.12	−1.86	−2.92	−0.45	−2.85	−1.85
G	−2.67	−4.83	−3.21	−4.15	−0.74	−3.61	−3.04

I-Mutant

	I108	M114	M213	L294	S362	I364	Y482
F	−0.91	0.43	0.50	−0.74	−0.30	−1.65	−0.31
Y	−1.98	−0.13	−0.78	−1.51	−1.03	−3.09	0.00
W	−2.31	−0.63	−0.59	−1.17	−0.36	−2.13	−0.47
H	−1.05	−1.85	−1.57	−2.82	−1.11	−2.33	−0.65
K	−2.26	−1.07	−1.12	−3.36	−1.14	−3.06	−0.78
D	−2.91	−0.44	0.43	−3.63	0.16	−1.69	−0.62
R	−2.01	−1.24	−0.89	−2.46	−1.02	−2.02	−1.03
E	−1.91	−0.47	−0.36	−2.22	−0.81	−1.69	−0.79
C	−2.78	−0.71	−0.13	−3.08	−1.87	−3.07	0.25
S	−2.44	−1.22	−1.15	−3.33	0.00	−2.51	−3.04
T	−2.61	−0.74	−0.10	−3.73	−0.84	−2.21	−1.03
Q	−2.24	−1.23	−1.58	−2.57	−1.26	−2.55	−1.39
N	−2.93	−0.86	−1.39	−3.15	−1.22	−1.75	−1.91
M	−0.95	0.00	0.00	−0.30	−0.61	−1.59	−0.97
P	−2.54	−0.83	−1.64	−1.77	−0.86	−2.40	−1.51
I	0.00	−0.58	−1.07	−1.26	−0.17	0.00	−0.94
V	−1.16	−1.01	−0.75	−1.16	−0.15	−0.95	−0.02
L	0.32	−0.20	−1.11	0.00	−0.85	−0.61	0.19
A	−3.06	−0.98	−0.76	−4.23	−1.32	−3.24	−2.46
G	−3.93	−2.63	−1.35	−5.24	−2.94	−4.54	−4.38

Figure S1. The ΔΔG value of all mutations (7x19) calculated by FoldX and I-Mutant.

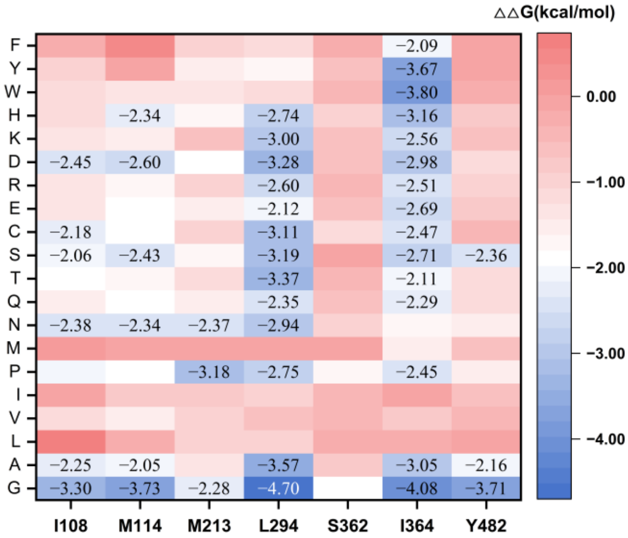

	I108	M114	M213	L294	S362	I364	Y482
F						−2.09	
Y						−3.67	
W						−3.80	
H		−2.34		−2.74		−3.16	
K				−3.00		−2.56	
D	−2.45	−2.60		−3.28		−2.98	
R				−2.60		−2.51	
E				−2.12		−2.69	
C	−2.18			−3.11		−2.47	
S	−2.06	−2.43		−3.19		−2.71	−2.36
T				−3.37		−2.11	
Q				−2.35		−2.29	
N	−2.38	−2.34	−2.37	−2.94			
M							
P			−3.18	−2.75		−2.45	
I							
V							
L							
A	−2.25	−2.05		−3.57		−3.05	−2.16
G	−3.30	−3.73	−2.28	−4.70		−4.08	−3.71

Figure S2. The 46 mutations with ΔΔG value less than -2.0 kcal/mol.

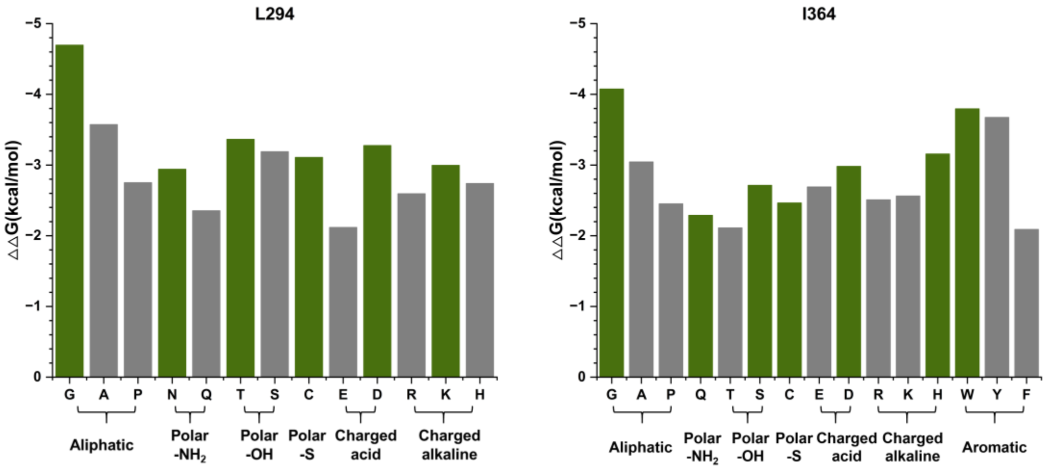

Figure S3. Mutations at L294 and I364 site with different residue properties was screened.

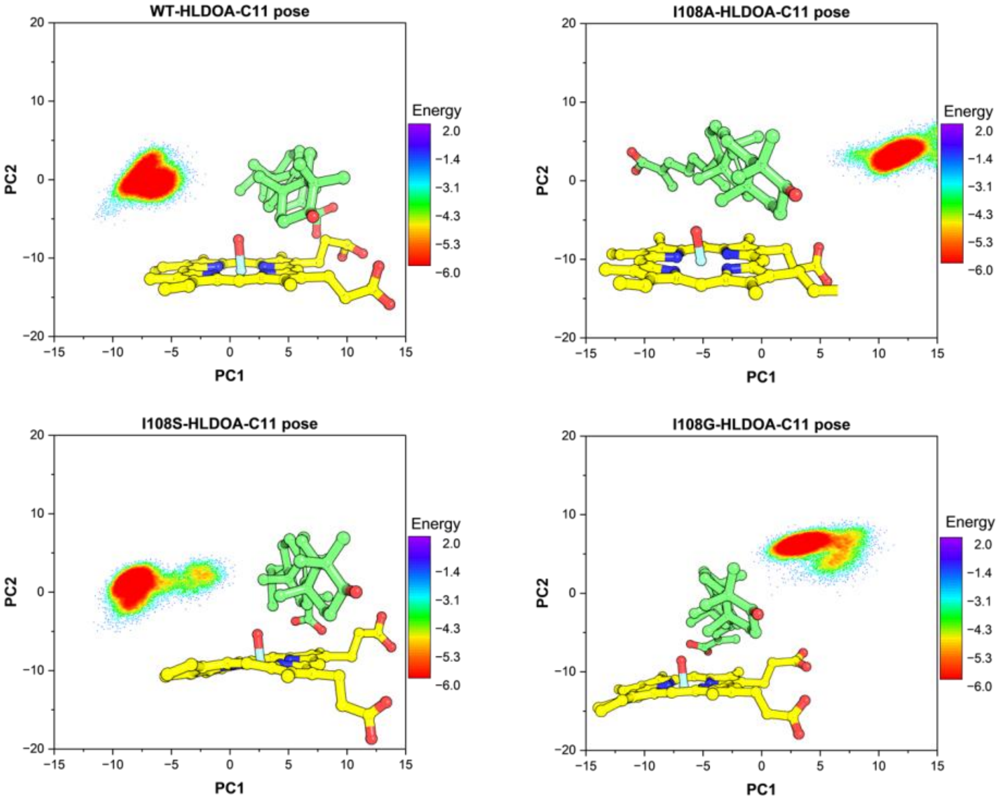

Figure S4. The PCA results of C11-HLDOA-WT/I108A/S/G models. The lowest energy conformations in variants I108A/S/G are showed.

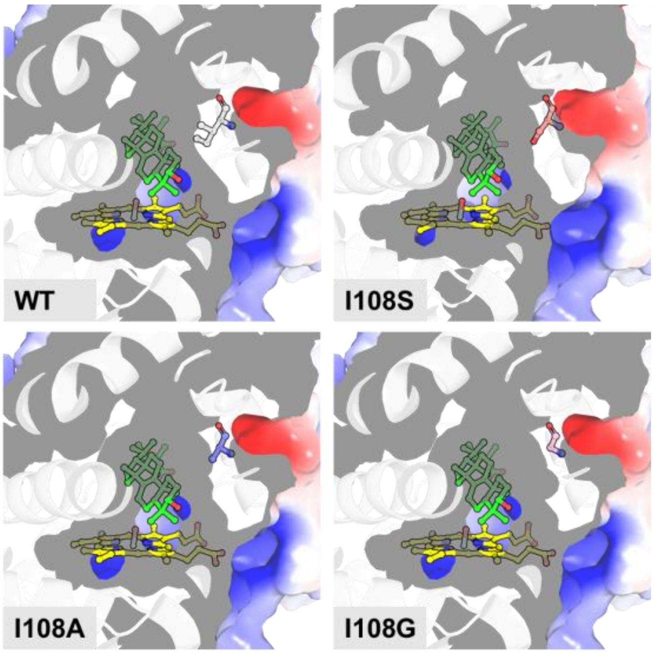

Figure S5. The active pocket of WT and variants I108A/S/G. For comparison purposes, all substrate conformations are the initial conformation of the substrates in WT. The pocket volumes enlarge in mutations.

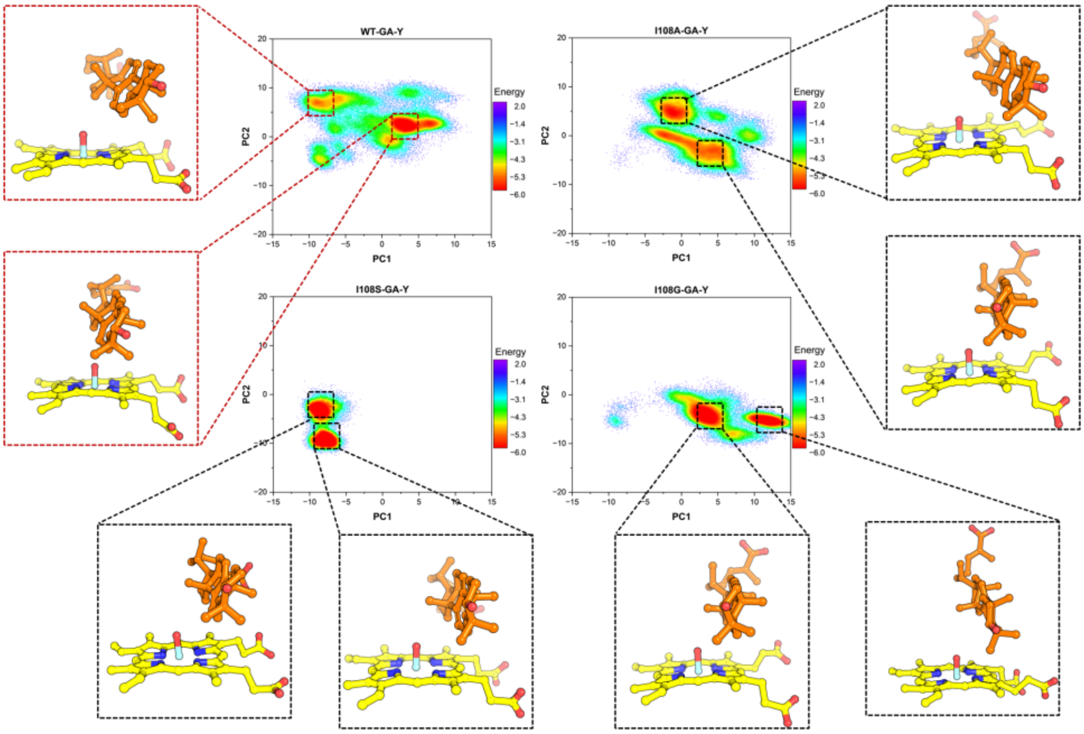

Figure S6. The PCA results of the substrate GA-Y in WT and variants I108A/S/G and the corresponding representative conformations (circled by red square in WT and black square in variants I108A/S/G).

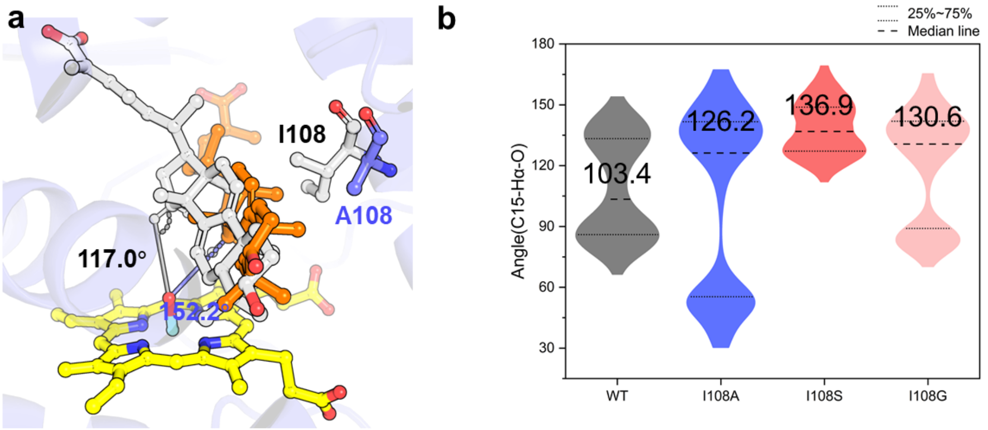

Figure S7. Comparative analysis of GA-Y substrate conformation and C15-Hα-O angular distribution. (a) The comparison of representative conformations of substrate GA-Y in WT and variant I108A. The Hα of C15 site in substrate GA-Y was showed by sticks and the angle (C15-Hα-O) was showed by solid line (gray in WT and violet in I108A). (b) Distributions of the angle (C15-Hα-O) in the MD simulations of WT and variants I108A/S/G.

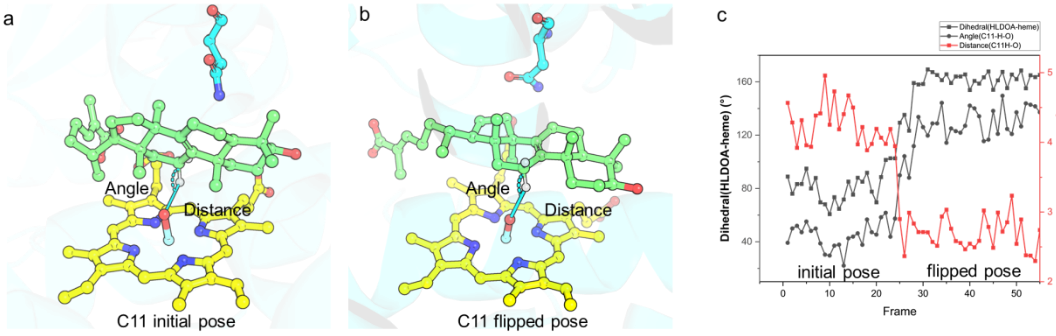

Figure S8. Binding mode of HLDOA substrates in C11-HLDOA-I108N model and dynamic analysis of key parameters. (a) The initial binding modes of substrate HLDOA in C11-HLDOA-I108N model. (b) The flipped binding modes of substrate HLDOA in C11-HLDOA-I108N model. (c) Change of the dihedral angle, the angle (C11-H-O) and the distance from C11H to O(-heme) during the first 100 ps in the MD simulations of C11-HLDOA-I108N model.

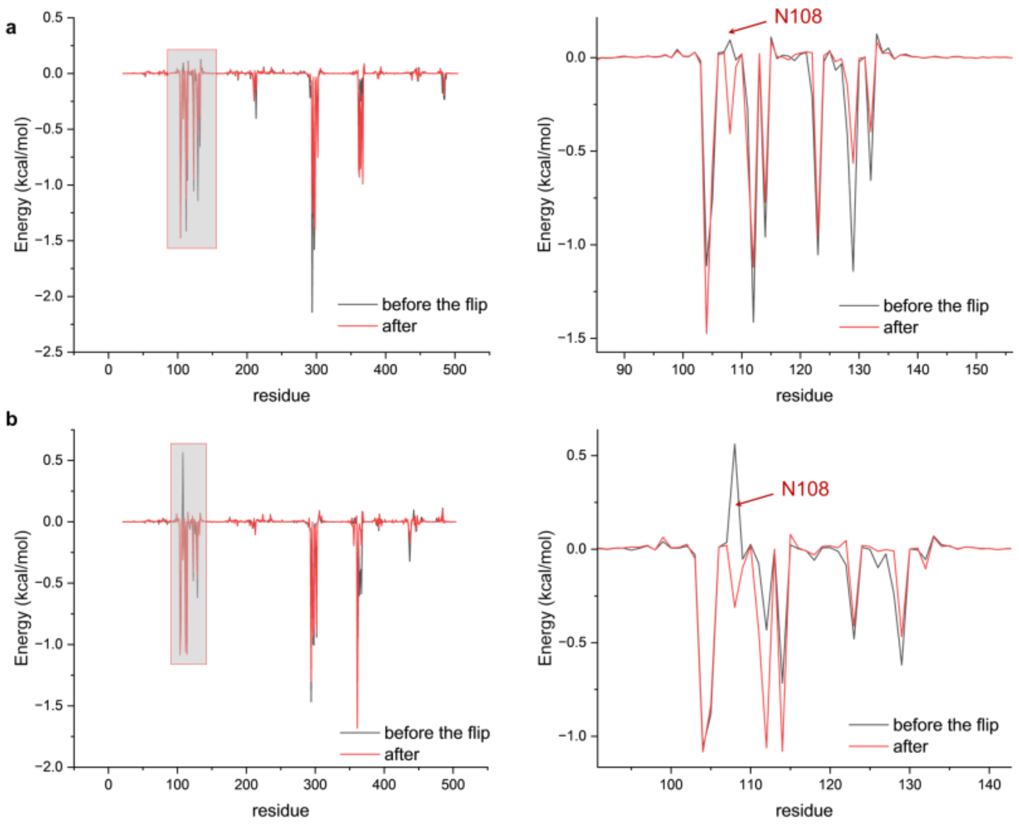

Figure S9. The energy decomposition analysis of (a) the C7-HLDOA-I108N model and (b) the C11-HLDOA-I108N model.

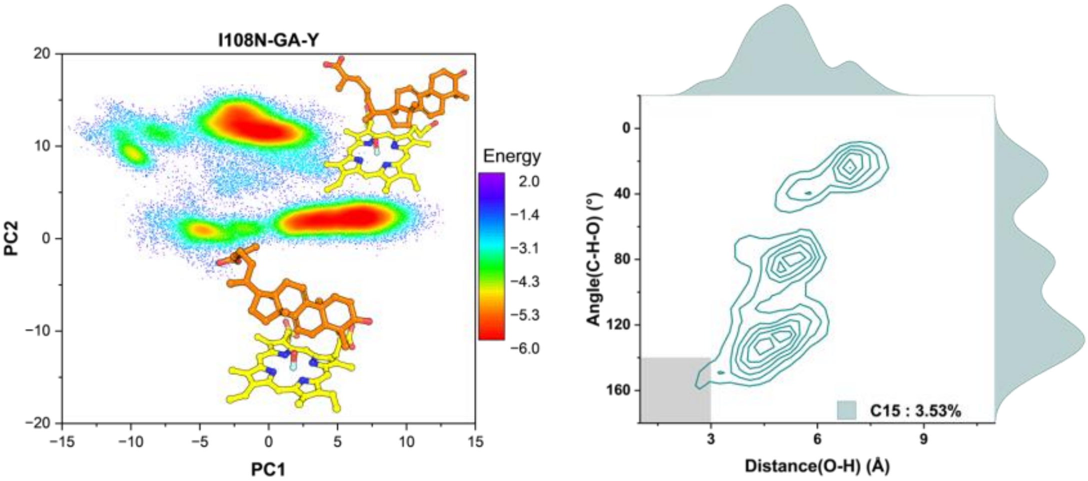

Figure S10. The PCA results of the substrate GA-Y in variant I108N and the PRSs occupancy of C15 site of GA-Y in variant I108N.

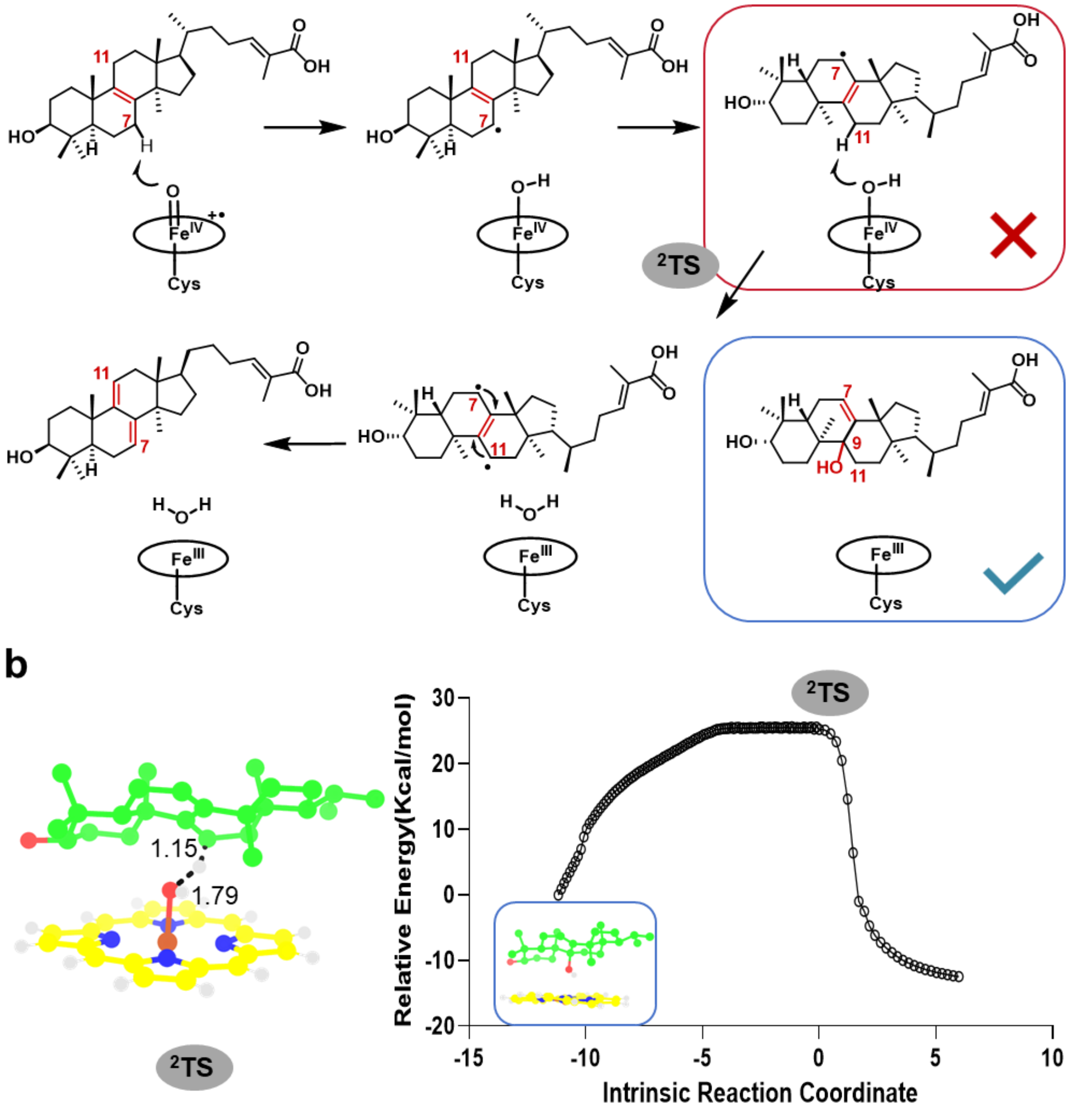

Figure S11 Computational analysis of the C7 radical intermediate in the I108N mutant. (a) Proposed alternative reaction pathway involving conformational flipping of the C7 radical intermediate for direct C11 hydrogen abstraction. (b) Intrinsic reaction coordinate (IRC) calculations showing that the C7 radical intermediate is unstable and reverts to the hydroxyl-rebound pathway, ruling out the hypothesized C11-abstraction mechanism.

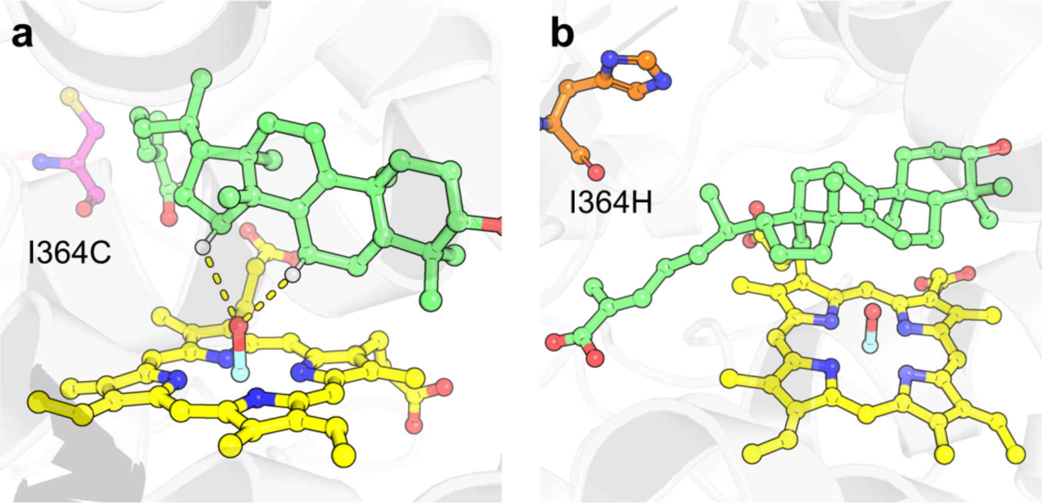

Figure S12 The major cluster conformations of (a) I364C and (b) I364H in complex with substrate HLDOA.

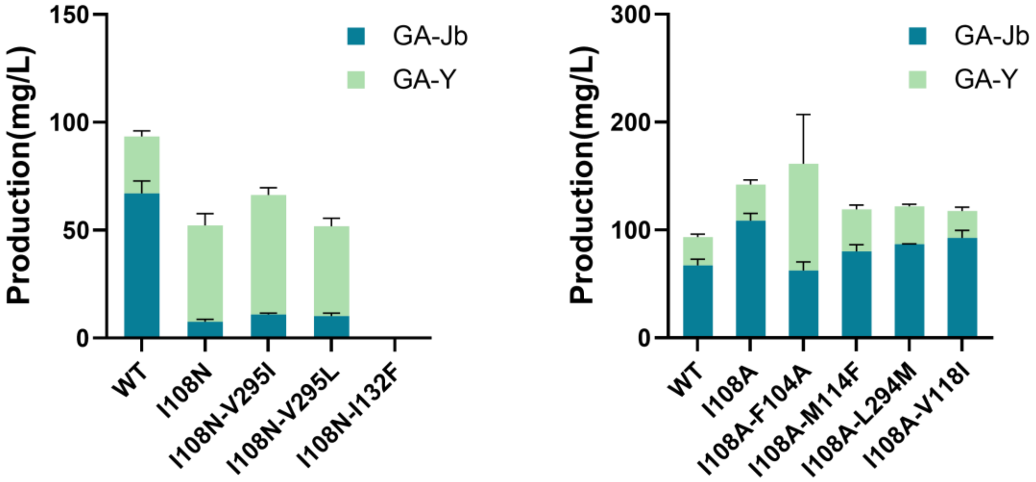

Figure S13 The yields and product ratios of the combinatorial mutagenesis by shake flask fermentation of strains for 120 h.

Supporting Tables

Table S1. The binding energy and C-O(heme) distance of CYP512W2 variants' docking results.

Mutants	**C11 POSE**		**C7 POSE**		
	Binding Energy(Kcal/mol)	**d(C11-O(heme)) (Å)**	**Binding Energy(Kcal/mol)**	**d(C7-O(heme)) (Å)**	**d(C15-O(heme)) (Å)**
I108A*	-12.33	3.4	-12.41	2.9	3.6
I108G	-11.75	4.9	-11.92	3.1	2.9
I108C	-12.7	3.7	-12.84	2.9	3.0
I108S	-12.84	3.8	**-12.98**	**2.9**	**2.7**
I108D	-12.73	4.7	-12.73	2.7	2.8
I108N	**-13.41**	**3.4**	-12.13	2.5	2.8
M114A*	-13.51	3.7	-13.11	2.7	2.7
M114G	-13.47	4.0	-13.12	2.9	2.7
M114N	-13.27	3.6	-12.91	2.9	2.8
M114S	-12.54	3.5	-12.31	2.9	2.7
M114D	-13.07	3.3	-12.68	2.8	2.7
M114H	**-13.63**	**2.9**	**-13.18**	**2.9**	**2.6**
M213R*	**-13.85**	**4.1**	**-13.53**	**2.9**	**2.6**
M213G	-13.71	4.1	-13.47	3.0	2.6
M213N	-13.72	4.1	-13.53	3.0	2.6
M213P	-13.77	3.9	-13.45	2.9	2.7
L294A*	-13.19	4.5	-12.9	3.1	2.6
L294C	-12.67	**2.7**	-11.62	2.9	3.0
L294D	-13.14	2.9	-12.15	2.7	3.2
L294G	-13.13	2.9	-13.13	2.9	3.0
L294K	-12.67	3.8	-11.65	3.4	5.7
L294N	**-13.48**	4.4	**-13.71**	3.0	2.7
L294T	-12.9	3.7	-11.98	2.8	2.8
I364A*	-12.81	4.4	-12.91	2.7	2.8
I364C	**-12.81**	4.3	**-12.89**	2.7	2.8
I365D	-12.72	4.4	-12.78	2.7	2.8
I366G	-12.76	4.3	-12.83	2.7	2.8
I367H	**-13**	4.3	**-13.06**	2.7	2.8
I368Q	**-12.84**	4.3	**-12.91**	2.7	2.8
I369S	-12.8	4.3	-12.87	2.7	2.8
Y482F*	-13.68	3.9	-13.28	2.9	2.6
Y482A	-13.73	3.8	-13.48	2.9	2.8
Y482G	**-13.80**	3.7	**-13.64**	2.7	2.9
Y482S	-13.69	3.7	-13.61	2.7	2.9
Y482V	**-13.81**	3.5	**-13.64**	2.7	2.9

*Control group (Five mutants that can either influence the catalytic activity of CYP512W2 or alter the yield of products GA-Y and GA-Jb in previous experiments).

Table S2. Construction of plasmids.

Plasmids	Construction scheme	Primer [a]	Primer sequence (5'-3')	Source
pRS426-HXT7p-FBA1t-G418r	-	-	-	
pRS426-CYP512W2-G418r	-	-	-	
-	-	CYP512W2-Seq-F	GCCAATACTTCACAATGTT	This study
-	-	CYP512W2-Seq-R	TCATTTTGTCATTGACCTT	This study
pRS426-I108C-G418r	I108C mutant fragments 1 and 2 were cloned by primer pairs CYP512W2-F and I108C-R, I108C-F and CYP512W2-R using plasmid pRS426-CYP512W2-G418r as template. PmeI linearized plamisd pRS426-HXT7p-FBA1t-G418r was ligated with I108C mutant fragments 1 and 2 to produce plasmid pRS426-I108C-G418r.	CYP512W2-F	TAATTTTAATCAAAAAGTTTATGGCG	This study
		I108C-R	GACTACTTCTTCACAGCCCTCCAAGAACGATA	
		I108C-F	TGTGAAGAAGTAGTCCACAT	
		CYP512W2-R	ATTAATTTGAATTAACGTTTTCAAGA	
pRS426-I108N-G418r	I108N mutant fragments 1 and 2 were cloned by primer pairs CYP512W2-F and I108N-R, I108N-F and CYP512W2-R using plasmid pRS426-CYP512W2-G418r as template. PmeI linearized plamisd pRS426-HXT7p-FBA1t-G418r was ligated with I108N mutant fragments 1 and 2 to produce plasmid pRS426-I108N-G418r.	CYP512W2-F	TAATTTTAATCAAAAAGTTTATGGCG	This study
		I108N-R	GACTACTTCTTCATTGCCCTCCAAGAACGATA	
		I108N-F	AATGAAGAAGTAGTCCACAT	
		CYP512W2-R	ATTAATTTGAAATTAACGTTTTCAAGA	
pRS426-I108S-G418r	I108S mutant fragments 1 and 2 were cloned by primer pairs CYP512W2-F and I108S-R, I108S-F and CYP512W2-R using plasmid pRS426-CYP512W2-G418r as template.	CYP512W2-F	TAATTTTAATCAAAAAGTTTATGGCG	This study
		I108S-R	GACTACTTCTTCATTGCCCTCCAAGAACGATA	
		I108S-F	AATGAAGAAGTAGTCCACAT	

	PmeI linearized plamisd pRS426-HXT7p-FBA1t-G418r was ligated with I108S mutant fragments 1 and 2 to produce plasmid pRS426-I108S-G418r.	CYP512W2-R	ATTAATTTGAATTAACGTTTTCAAGA	
pRS426-I108G-G418r	I108G mutant fragments 1 and 2 were cloned by primer pairs CYP512W2-F and I108G-R, I108G-F and CYP512W2-R using plasmid pRS426-CYP512W2-G418r as template. PmeI linearized plamisd pRS426-HXT7p-FBA1t-G418r was ligated with I108G mutant fragments 1 and 2 to produce plasmid pRS426-I108G-G418r.	CYP512W2-F	TAATTTTAATCAAAAAGTTTATGGCG	This study
		I108G-R	ATGTGGACTACTTCTTCACCGCCCTCCAAGAACGATA	
		I108G-F	GGTGAAGAAGTAGTCCACAT	
		CYP512W2-R	ATTAATTTGAATTAACGTTTTCAAGA	
pRS426-I108D-G418r	I108D mutant fragments 1 and 2 were cloned by primer pairs CYP512W2-F and I108D-R, I108D-F and CYP512W2-R using plasmid pRS426-CYP512W2-G418r as template. PmeI linearized plamisd pRS426-HXT7p-FBA1t-G418r was ligated with I108D mutant fragments 1 and 2 to produce plasmid pRS426-I108D-G418r.	CYP512W2-F	TAATTTTAATCAAAAAGTTTATGGCG	This study
		I108D-R	ATGTGGACTACTTCTTCATCGCCCTCCAAGAACGATA	
		I108D-F	GATGAAGAAGTAGTCCACAT	
		CYP512W2-R	ATTAATTTGAATTAACGTTTTCAAGA	
pRS426-M114H-G418r	M114H mutant fragments 1 and 2 were cloned by primer pairs CYP512W2-F and M114H-R, M114H-F and CYP512W2-R using plasmid pRS426-CYP512W2-G418r as template. PmeI linearized plamisd pRS426-HXT7p-FBA1t-G418r was ligated with M114H mutant fragments 1 and 2 to produce plasmid pRS426-M114H-G418r.	CYP512W2-F	TAATTTTAATCAAAAAGTTTATGGCG	This study
		M114H-R	GACAGTGTACTTATGGTGGACTACTTCTTCAA	
		M114H-F	CATAAGTACACTGTCGGGC	
		CYP512W2-R	ATTAATTTGAATTAACGTTTTCAAGA	

pRS426-L294C-G418r	L294C mutant fragments 1 and 2 were cloned by primer pairs CYP512W2-F and L294C-R, L294C-F and CYP512W2-R using plasmid pRS426-CYP512W2-G418r as template. PmeI linearized plamisd pRS426-HXT7p-FBA1t-G418r was ligated with L294C mutant fragments 1 and 2 to produce plasmid pRS426-L294C-G418r.	CYP512W2-F	TAATTTTAATCAAAAAGTTTATGGCG	This study
		L294C-R	TGCAAAGTTGACACAGAATATTCGCTCGACGA	
		L294C-F	TGTGTCAACTTTGCAGC	
		CYP512W2-R	ATTAATTTGAATTAACGTTTTCAAGA	
pRS426-L294N-G418r	L294N mutant fragments 1 and 2 were cloned by primer pairs CYP512W2-F and L294N-R, L294N-F and CYP512W2-R using plasmid pRS426-CYP512W2-G418r as template. PmeI linearized plamisd pRS426-HXT7p-FBA1t-G418r was ligated with L294N mutant fragments 1 and 2 to produce plasmid pRS426-L294N-G418r.	CYP512W2-F	TAATTTTAATCAAAAAGTTTATGGCG	This study
		L294N-R	TGCAAAGTTGACATTGAATATTCGCTCGACGA	
		L294N-F	AATGTCAACTTTGCAGCC	
		CYP512W2-R	ATTAATTTGAATTAACGTTTTCAAGA	
pRS426-I364C-G418r	I364C mutant fragments 1 and 2 were cloned by primer pairs CYP512W2-F and I364C-R, I364C-F and CYP512W2-R using plasmid pRS426-CYP512W2-G418r as template. PmeI linearized plamisd pRS426-HXT7p-FBA1t-G418r was ligated with I364C mutant fragments 1 and 2 to produce plasmid pRS426-I364C-G418r.	CYP512W2-F	TAATTTTAATCAAAAAGTTTATGGCG	This study
		I364C-R	TGCGCATCAGGCCACAGAGGGAGATCCCGTGGTACC	
		I364C-F	TGTGGCCTGATGCGCAAGTCCGT	
		CYP512W2-R	ATTAATTTGAATTAACGTTTTCAAGA	
pRS426-I364H-G418r	I364H mutant fragments 1 and 2 were cloned by primer pairs CYP512W2-F and I364H-R, I364H-F and CYP512W2-R	CYP512W2-F	TAATTTTAATCAAAAAGTTTATGGCG	This study
		I364H-R	TGCGCATCAGGCCATGGAGGGAGATCCCGTGGTACC	

	using plasmid pRS426-CYP512W2-G418r as template. PmeI linearized plamisd pRS426-HXT7p-FBA1t-G418r was ligated with I364H mutant fragments 1 and 2 to produce plasmid pRS426-I364H-G418r.	I364H-F	CATGGCCTGATGCGCAAGTCCGT	
		CYP512W2-R	ATTAATTTGAATTAACGTTTTCAAGA	
pRS426-I364Q-G418r	I364Q mutant fragments 1 and 2 were cloned by primer pairs CYP512W2-F and I364Q-R, I364Q-F and CYP512W2-R using plasmid pRS426-CYP512W2-G418r as template. PmeI linearized plamisd pRS426-HXT7p-FBA1t-G418r was ligated with I364Q mutant fragments 1 and 2 to produce plasmid pRS426-I364Q-G418r.	CYP512W2-F	TAATTTTAATCAAAAAGTTTATGGCG	This study
		I364Q-R	TGCGCATCAGGCCTTGGAGGGAGATCCCGTGGTACC	
		I364Q-F	CAAGGCCTGATGCGCAAGTCCGT	
		CYP512W2-R	ATTAATTTGAATTAACGTTTTCAAGA	
pRS426-Y482V-G418r	Y482V mutant fragments 1 and 2 were cloned by primer pairs CYP512W2-F and Y482V-R, Y482V-F and SacII-R using plasmid pRS426-CYP512W2-G418r as template. PmeI and SacII linearized plamisd pRS426-HXT7p-FBA1t-G418-r was ligated with Y482V mutant fragments 1 and 2 to produce plasmid pRS426-Y482V-G418r.	CYP512W2-F	TAATTTTAATCAAAAAGTTTATGGCG	This study
		Y482V-R	GACGTTCGTGCCAACGTAAAAGTTCGCCGGCC	
		Y482V-F	GTTGGCACGAACGTCGT	
		SacII-R	AAGCTGGAGCTCCACCGCGG	
pRS426-Y482G-G418r	Y482G mutant fragments 1 and 2 were cloned by primer pairs CYP512W2-F and Y482G-R, Y482G-F and SacII-R using plasmid pRS426-CYP512W2-G418r as template. PmeI and SacII linearized plamisd pRS426-HXT7p-FBA1t-G418-r was ligated with Y482G mutant fragments 1 and 2 to	CYP512W2-F	TAATTTTAATCAAAAAGTTTATGGCG	This study
		Y482G-R	GACGTTCGTGCCACCGTAAAAGTTCGCCGGCC	
		Y482G-F	GGTGGCACGAACGTCGT	
		SacII-R	AAGCTGGAGCTCCACCGCGG	

	produce plasmid pRS426-Y482G-G418r.	

Table S3. Strains used in this study.

Strains	**Description**	**Source**
E. coli DH5α	General cloning host.	TaKaRa, Japan
SC62	YL-T3-rDNA::eGFP-TRP1-CYP5150L8-iGLCPR.	[12]
SC62-CK	SC62 harboring plasmid pRS426-HXT7p-FBA1t-G418r.	This study
SC62-WT	SC62 harboring plasmid pRS426-CYP512W2-G418r.	This study
SC62-I108S	SC62 harboring plasmid pRS426-I108S-G418r.	This study
SC62-I108N	SC62 harboring plasmid pRS426-I108N-G418r.	This study
SC62-I108C	SC62 harboring plasmid pRS426-I108C-G418r.	This study
SC62-I108G	SC62 harboring plasmid pRS426-I108G-G418r.	This study
SC62-I108D	SC62 harboring plasmid pRS426-I108D-G418r.	This study
SC62-M114H	SC62 harboring plasmid pRS426-M114H-G418r.	This study
SC62-L294C	SC62 harboring plasmid pRS426-L294C-G418r.	This study
SC62-L294N	SC62 harboring plasmid pRS426-L294N-G418r.	This study
SC62-I364C	SC62 harboring plasmid pRS426-I364C-G418r.	This study
SC62-I364H	SC62 harboring plasmid pRS426-I364H-G418r.	This study
SC62-I364Q	SC62 harboring plasmid pRS426-I364Q-G418r.	This study
SC62-Y482V	SC62 harboring plasmid pRS426-Y482V-G418r.	This study
SC62-Y482G	SC62 harboring plasmid pRS426-Y482G-G418r.	This study

Table S4. Product ratio of Diverse Mutants to Generate GA-Jb and GA-Y.

	Product ratio of GA-Jb / GA-Y (%) [a]			
	48 h	72 h	96 h	120 h
WT	70.7/29.3	70.2/29.8	72.7/27.3	76.4/23.6
I108S	46.7*** / 53.3***	59.8*** / 40.2***	61.7*** / 38.3***	63.2*** / 36.8***
I108N	9.6*** / 90.4%***	11.1*** / 88.9***	16.9*** / 83.1***	20.8*** / 79.2***
M114H	36.9*** / 63.1***	48.9*** / 51.1***	48.1*** / 51.9***	50.3*** / 49.7***
L294C	64.9*** / 35.1***	72.0* / 28.0*	73.9** / 26.1	75.0** / 25.0
L294N	53.9*** / 46.1***	66.1 / 33.9	68.3** / 31.7**	70.5** / 29.5**
I364H	8.3*** / 91.7***	12.2*** / 87.8***	13.4*** / 86.6***	14.6*** / 85.4***
I364C	64.5*** / 35.5***	72.0* / 28.0*	75.8* / 24.2*	77.0 / 23.0
I364Q	14.1*** / 85.9***	18.7*** / 81.3***	20.8*** / 79.2***	22.3*** / 77.7***
Y482V	56.8*** / 43.2***	64.8*** / 35.2***	67.0** / 33.0**	68.7*** / 31.3***
Y482G	60.4*** / 39.6***	67.5** / 32.5**	67.9** / 32.1**	70.6** / 29.4**
I108A	63.9*** / 36.1***	74.0** / 26.0**	81.1*** / 18.9***	84.8*** / 15.2***
I108C	55.5** / 44.5**	62.5*** / 37.5***	60.7*** / 39.3***	60.1*** / 39.9***
I108D	0.0*** / 0.0***	0.0*** / 100.0***	0.0*** / 100.0***	0.0*** / 100.0***
I108G	40.4*** / 59.6***	47.4** / 52.6**	50.9*** / 49.1***	52.0*** / 48.0***
	Production of GA-Jb / GA-Y as compared with SC62-WT[b]			
	48 h	72 h	96 h	120 h
WT	1.00 / 1.00	1.00 / 1.00	1.00 / 1.00	1.00 / 1.00
I108S	0.53*** / 1.46*	1.21 / 1.92***	1.50*** / 2.48***	1.30** / 2.45***
I108N	0.04*** / 0.83	0.09** / 1.74**	0.20*** / 2.56***	0.20*** / 2.50***
M114H	0.23*** / 0.95	0.59** / 1.46*	0.70*** / 1.99***	0.65*** / 1.46***
L294C	0.77** / 1.01	1.30* / 1.20	1.38*** / 1.30*	1.27*** / 1.37*
L294N	0.52*** / 1.08*	1.21 / 1.47*	1.17 / 1.45*	1.14 / 1.56*
I364H	0.03*** / 0.88	0.10** / 1.67***	0.13*** / 2.28***	0.13*** / 2.51***
I364C	0.66** / 0.88	1.21 / 1.12	1.39** / 1.19	1.33*** / 1.29*
I364Q	0.04*** / 0.71	0.12** / 1.28	0.18*** / 1.89	0.16*** / 1.89
Y482V	0.68** / 1.24*	1.19 / 1.53*	1.20 / 1.57*	1.08 / 1.59**
Y482G	0.63** / 1.00	1.19 / 1.36**	1.22* / 1.54**	1.03 / 1.38**
I108A	0.68** / 0.93	1.12 / 0.93	1.80*** / 1.11	1.77** / 1.03
I108C	0.59** / 1.14	1.15 / 1.64**	1.44** / 2.47***	1.12* / 2.42***
I108D	0.00*** / 0.02***	0.00** / 0.07***	0.00*** / 0.12***	0.00*** / 0.12**
I108G	0.39*** / 1.41*	0.85 / 2.26**	1.22 / 3.13***	0.95 / 2.87**

[a] Product ratio of GA-Jb or GA-Y titers in the total titers of GA-Jb and GA-Y. [b] Production of GA-Jb/GA-Y as compared with SC62-WT refers to the ratio of the GA-Jb/Y production titer of the mutant to that of the WT. *$p < 0.05$; **$p < 0.01$; ***$p < 0.001$.

Table S5. The percentage of PRSs in three MD simulations in WT and its variants I108A/S/G.

	C7 pose (%)			**C11 pose (%)**			**C15 pose(%)**		
	$H\alpha_{C7}$	**$H\beta_{C7}$**	**total**	**$H\alpha_{C11}$**	**$H\beta_{C11}$**	**total**	**$H\alpha_{C15}$**	**$H\beta_{C15}$**	**total**
WT	5.4	7.7	13.1	0.0	9.0	9.0	10.8	0.4	11.2
I108A	22.5	5.1	27.6	0.1	13.6	13.7	18.9	1.4	20.3
I108S	15.8	1.1	16.9	0.0	9.7	9.7	24.7	0.0	24.7
I108G	20.2	1.3	21.5	4.3	6.8	11.1	13.6	0.0	13.6

Table S6. The binding energy of CYP512W2 mutants calculated by MM/GBSA.

Systems	**Binding Energy(kcal/mol)**
WT-GA-Y	-33.1±2.9
I108A-GA-Y	-36.6±4.5
I108S-GA-Y	-36.3±2.6
I108G-GA-Y	-38.8±3.7
I108N-GA-Y	-30.5±3.0